Available online at www.sciencedirect.com
ScienceDirect
Journal of Molecular Graphics and Modelling 26 (2007) 20–31
Journal of Molecular Graphics and Modelling
www.elsevier.com/locate/JMGM

Molecular modeling of purinergic receptor P2Y12 and interaction with its antagonists

Chenyang Zhan [a,b], Jie Yang [a,*], Xian-Chi Dong [a,c], Yue-Lan Wang [a]

[a] State Key Laboratory of Pharmaceutical Biotechnology, Life College, Nanjing University, Nanjing 210093, China
[b] Department of Biochemistry, Albert Einstein College of Medicine, 1300 Morris Park Avenue, Bronx, NY 10461, USA
[c] Key Laboratory of Proteomics, Institution of Biochemistry and Cell Biology, Shanghai Institutes for Biological Sciences, Chinese Academy of Sciences, 320 Yueyang Road, Shanghai 200031, China

Received 15 February 2006; received in revised form 18 September 2006; accepted 20 September 2006
Available online 26 September 2006

Abstract

Purinergic receptors are a class of cell surface receptors for purines that prefer ATP or ADP over adenosine. The surface receptors for extracellular nucleotides are called P2 receptors. They are activated by both pyrimidine and purine nucleotides. ADP initiates platelet aggregation by 'simultaneous activation of two G protein-coupled receptors, P2Y1 and P2Y12. P2Y12 has been shown to be the target of the thienopyridine drugs, ticlopidine and clopidogrel. Here, the active sites of P2Y12 for ATP as well as ADP are predicted by bioinformatics and molecular modeling. First, the three-dimensional (3D) structure of P2Y12 was constructed by InsightII/Homology module using the corresponding bovine rhodopsin (PDB code: 1HZX) as the template. Then the primary structures were optimized by energy minimization that has been successfully accepted by the Protein Data Bank (PDB code: 1VZ1). Second, a simple scoring matrix was built up based on the analysis of 13 known ATP-binding proteins. And the most probable active sites of P2Y12 were predicted using the scoring matrix, which include three distant areas: ''head area'' (LGTGPLRTFV, 87–96), ''middle area'' (VGLITNGLAM, 38–47, and LGAKILSVVI, 139–148), and ''bottom area'' (RTRGVGKVPR, 222–231). Subsequently the structural model of P2Y12 was docked with ATP/ADP in comparison with P2Y1 (PDB code 1ddd). As a comparison, we docked its antagonists, such as ticlopidine and clopidogrel, to the most probable sites and calculated their intermolecular energy. Our results imply that P2Y12 has the potential to be inhibited by ADP/ATP analogs, and it suggests that P2Y12 acts as a target of new drugs that inhibit platelet aggregation.

Keywords: P2Y12; ADP receptor; Antagonists; ATP; Platelets aggregation

1. Introduction

Purinergic receptors are a class of cell surface receptors for purines that prefer ATP or ADP over adenosine. The surface receptors for extracellular nucleotides are called P2 receptors. Previously they were called P2 purinoreceptors, but it is now realized that some P2 receptors are activated by both pyrimidine and purine nucleotides. The current nomenclature system for P2 receptors is based on molecular structure and signal transduction mechanisms. In this light, the families of ionotropic receptors (ligand-gated ion channels) and metabotropic receptors (G protein coupled receptors) are named as P2X and P2Y receptors, respectively. Forty years ago ADP was found to have an influence on platelet aggregation as well as their adhesion, which made it the most important medium in the whole process of the platelet and thrombosis. Twenty years later ticlopidine was found to be an antiplatelet medicine, which selectively inhibits the aggregation of platelet of ADP [1]. In the latest 10 years, more evidences have showed that ADP plays a critical role in modulating thrombosis and hemostasis. ADP initiates platelet aggregation by simultaneous activation of two G protein-coupled receptors, P2Y1 and P2Y12. Activation of P2Y1 activates phospholipase C and triggers shape change, while P2Y12 couples to Gi to reduce adenylyl cyclase activity. P2Y12 has been shown to be the target of the thienopyridine drugs, ticlopidine and clopidogrel [2,3].

Adenine nucleotides act on platelets through three distinct P2 receptors: two are G protein-coupled adenosine diphosphate (ADP) receptors, viz. the P2Y1 and P2Y12 receptor subtypes;

* Corresponding author at: Department of Biochemistry, Nanjing University, Nanjing 210093, China. Tel.: +86 25 8359 4060; fax: +86 25 8332 4605.
E-mail address: luckyjyj@sina.com.cn (J. Yang).

1093-3263/$ – see front matter © 2006 Elsevier Inc. All rights reserved.
doi:10.1016/j.jmgm.2006.09.006

and the ligand-gated cation channel P2X1 receptor, which is activated by adenosine triphosphate (ATP). P2Y1 receptor initiates platelet aggregation but is not sufficient for a full platelet aggregation in response to ADP, whereas P2Y12 receptor is responsible for completion of the aggregation to ADP. This receptor, the molecular target of the antithrombotic drug clopidogrel, is responsible for most effects of ADP when platelets are stimulated by agents such as thrombin, collagen, or immune complexes [4,5] ATP acting on both P2Y1 and P2Y2 receptors produced a transient Ca^{++} release [6], which is important for P2Y1 function, and leads to the shape alteration and temporal assemble of platelet; meanwhile, the P2Y12 takes part in strengthening the assemble and exudation of platelet; it is as well, the target of specific antiplatelet drugs, such as ticlopidine and AR-C complex [5]. The P2X1 receptor is involved in platelet shape change and in activation by collagen under shear conditions. And it takes charge in rapid calcium ion inside flowing in the cell, which may has a cooperation with P2Y1, of which the mechanism has not been well established by now [7]. Each of these receptors is coupled to specific signal transduction pathways in response to ADP or ATP and is differentially involved in all of the sequential events involved in platelet function and hemostasis.

Because of its central role in the formation and stabilization of a thrombus, the P2Y12 receptor is a well-established target of antithrombotic drugs such as clopidogrel, which has proven efficacy in many clinical trials and experimental models of thrombosis. Competitive P2Y12 antagonists have also been shown to be effective in experimental thrombosis as well as in several clinical trials [8]. It will be a great advantage for the discovery of novel antiplatelet drugs if we know the structure of P2Y12. However, as a membrane protein, it is very difficult to achieve this aim with experimental approaches. As an alternative, the quick development of molecular modeling methods has provided us with unprecedented power to investigation in both fundamental and industrial researches [9]. In this light, we focus on constructing 3D structural models for P2Y12 receptor and its complex with the ligands. Together with other ongoing researches, this paper proves that structural bioinformatics is a very powerful tool in investigating the interactions between purinergic receptors and their antagonists [10–13].

2. Materials and methods

2.1. The 3D structure modeling of P2Y12

Firstly, we used the NCBI PSI-BLAST to search for a template for the homologous modeling of P2Y12, Bovine rhodopsin (PDB code: 1HZX) [14], a seven trans-membrane protein, was shown to be the most proper template. The detailed result of their alignment performed by CLUSTAL will be listed in Table 1.

Then protein P2Y12 was modeled on the Silicon Graphics Iris Indigo XZ4000 (SGI Inc., Silicon, CA, USA) workstation with the *Homology* module of the software InsightII 2000

Table 1
The CLUSTAL alignment between P2Y12 and rhodopsin

```
p2y12          ----------MQAVDNLTSAPGNTSLCTRDYKITQVLFPLLYTVLFFVGLITNGLAMRIFF 51
rhodopsin      MNGTEGPNFYVPFSNKTGVVRSPFEAPQYYLAEPWQFSMLAAYMFLLIMLGFPINFLTLY 60
                          ...* *..  ..  ..: *      *.:* : :*:: ::   : :  ::
p2y12          QIRS----KSNFIIFLKNTVISDLLMILTFPFKILSDAKLGTGPLRTFVCQVTSVIFYFT 107
rhodopsin      VTVQHKKLRTPLNYILLNLAVADLFMVFGGFTTTLYTSLHGYFVFGPTGCNLEGFFATLG 120
                  .    :: :  :* * .::**:*::    . *  :  *   : .  *:: ..:  :
p2y12          MYISISFLGLITIDRYQKTTRPFKTSNPKNLLGAKILSVVIWAFMFLLSLPNMILTNRQP 167
rhodopsin      GEIALWSLVVLAIERYVVVCKPMSNFR-FGENHAIMGVAFTWVMALACAAPPLVGWSRYI 179
                 *::  * :::*:**  . :*:.. .  .   * :  .. *.: :  : * ::  .*
p2y12          RDKNVKKC--SFLKSEFGLVWHEIVNYICQVIFWINFLIVIVCYTLITKELYRSYVRTR- 224
rhodopsin      PEGMQCSCGIDYYTPHEETNNESFVIYMFVVHFIIPLIVIFFCYGQLVFTVKEAAAQQQE 239
                :    .*  .: ...     ..:* *:  * * * :::::.**  :.  : .: .: :
p2y12          -GVGKVPRKKVNVKVFIIIAVFFICFVPFHFARIPYTLSQTRDVFDCTAENTLFYVKEST 283
rhodopsin      SATTQKAEKEVTRMVIIMVIAFLICWLPYAGVAFYIFTHQGSDFGPIFMTIPAFFAKTS- 298
                .. : ..*:*.  *:*:: .*:**::*:  . :     *  *.       . *:.* *
p2y12          LWLTSLNACLDPFIYFFLCKSFRNSLISMLKCPNSATSLSQDNRKKEQDGGDPNEETPM 342
rhodopsin      -------AVYNPVIYIMMNKQFRNCMVTTLCCG--KNPLGDDEASTTVSKTETSQVAPA 348
                     *  :*.**::: *.***.::: * *    ..*.:*: ..  .  :..: :*
```

Note: The marks "*", ".", and ":" stand for the identical amino acids, relative, and similar amino acids, respectively.

Table 2
The ATP-binding sites in 13 proteins

Protein (PDB code)		Sequence		Name of the proteins	Ref.
1HCK	10	IGEGTYGVVY	19	human cyclin-dependent kinase 2	21
1ATP	49	LGTGSFGRVM	58	cAMP-dependent protein-kinase	22
1PHK	25	LGRGVSSVVR	34	phosphorylase kinase	23
1A82	10	DTEVGKTVAS	19	ATP-dependent enzyme dethiobiotin synthetase	24
1CSN	18	IGEGSFGVIF	27	casein kinase-1	25
1MJH	10	YPTDFSETAE	19	hypothetical protein MJ0577	26
1A49	72	RMNFSHGTHE	81	rabbit muscle pyruvate kinase	27
1AYL	250	SGTGKTTLST	259	PEP carboxykinase	28
1B8A	214	RAEEHNTTRH	223	aspartyl-tRNA synthetase	29
1KAY	11	LGTTYSCVGV	20	chaperone protein Hsc70	30
1E8X	662	VMASKKKPLW	671	phosphoinositide 3-kinase	31
1YAG	12	NGSGMCKAGF	21	nonvertebrate actin	32
1NSF	29	YIWNGIIKWG	38	N-ethylmaleimide sensitive factor	33

(Biosym Technologies Inc., San Diego, CA, USA) using a template as bovine rhodopsin (1HZX) based on our previous works [15–17]. The best fitting loops were chosen to construct the non-paried sequence. Some modification was made after examination of the electric charge in the *Biopolymer* module. In the *Discover* module the energy minimization was executed. We have adopted the ''steepest'' 2000 steps, then 5000 steps of the ''conjugate''; as soon as the RMS was below 0.001. Then we did Dynamics calculation 100,000 steps to get a more reliable structure. At last, it has been saved as PDB form and submitted to the Protein Data Bank, whose PDB code is 1VZ1.

2.2. Sequence analysis of P2Y12 receptor using bioinformatics

In order to represent the ATP binding patterns, a representative non-redundant set of high resolution ATP-containing structures are chosen as previously reported [18]. They are listed as: 1HCK (human cyclin-dependent kinase 2) [19], 1ATP (cAMP-dependent protein-kinase) [20], 1PHK (phosphorylase kinase) [21], 1A82 (ATP-dependent enzyme dethiobiotin synthetase) [22], 1CSN (casein kinase-1) [23], 1MJH (hypothetical protein MJ0577) [24], 1A49 (rabbit muscle pyruvate kinase) [25], 1AYL (PEP carboxykinase) [26], 1B8A (aspartyl-tRNA synthetase) [27], 1KAY (chaperone protein Hsc70) [28], 1E8X (phosphoinositide 3-kinase) [29], 1YAG (non-vertebrate actin) [30], and 1NSF (*N*-ethylmaleimide sensitive factor) [31], respectively, which contains ATP-binding sites whether they are kinase or not (Table 2). The most consistent sequences are picked up to constitute a scoring matrix that would be used to predict the ATP active site. Using the LPC, the 13 proteins' ATP binding sites are determined. For all the proteins, the active sites cluster in one or two fragments which are about 10 amino acid long. Therefore, such fragments of 10 amino acids are chosen to

Table 3
Each amino acids' score in each position

Residues	Position									
	1	2	3	4	5	6	7	8	9	10
I	2	1	0	0	0	1	1	0	1	0
L	3	0	0	0	0	0	0	1	1	0
D	1	0	0	1	0	0	0	0	0	0
Y	2	0	0	0	1	1	0	0	0	1
R	2	0	1	0	0	0	0	1	1	1
S	1	0	1	1	3	3	1	0	1	1
V	1	0	0	1	1	0	0	5	3	1
N	1	0	1	1	0	1	0	0	0	0
G	0	7	0	6	2	0	4	0	2	1
T	0	1	4	1	1	1	3	3	0	1
P	0	1	0	0	0	0	0	1	0	0
M	0	2	1	0	1	0	0	0	0	1
A	0	1	1	0	0	0	0	1	2	0
E	0	0	4	1	0	0	1	0	0	2
F	0	0	0	1	1	2	0	0	0	2
K	0	0	0	0	2	2	2	1	0	0
H	0	0	0	0	1	1	0	0	1	1
C	0	0	0	0	0	1	1	0	0	0
W	0	0	0	0	0	0	0	0	1	1

constitute the scoring matrix, which contains 19 types of amino acid residues except of glutamine (Gln, Q).

Table 3 means the scoring matrix, which was generated by assigning a value of the stimulatory potential to each of the 19 defined amino acids in each position of Table 2. Based on the matrix, we designed a simple algorithm to evaluate the relationship significance of any sequence to the ATP binding patterns. To each amino acid a (I, L, D, ..., W) from those 13 proteins, the score Sij stands for how many times it takes place in each position $j(j \in 1, 2, 3, \ldots, 10)$, which was calculated as follows: $Sij = \sum\sum_{i=1}^{13} aij$. Take the isoleucine (Ile, I) for example. Based on the Table 2, the score of this residue is 2, 1, 1, 1, and 1 at the position of 1, 2, 6, 7, and 9, respectively, whereas it is 0 at other position because it does not appear. And the value of the scoring matrix is 120.

Based on the matrix constructed by Sij, we designed a program for the prediction of ATP binding protein. Suppose that independent sequences contribute to stimulation, the predicted stimulatory potential of given peptide is the sum of amino acid's scores in each position. Some 10-residue sequences can be scored as follows by the matrix (Table 3) mentioned above:$S = \sum_{j=1}^{10} Sij$. Here, when some amino acid (using the same order as for the rows of the scoring matrix) is in position j, its score is Sij at the different position. As to the whole fragment sequence, the score is the sum of scores of its all amino acids. For example, the total score of 10-residue motif GAKILSVVIW is 11. And 10-residue units are obtained using the sliding window method one by one from N-terminal of protein sequences to C-teminal: a sequence of n residues gives rise to $n - 9$ 10-peptide units. Therefore, a 10-peptide sequence could be pick out for its highest score, which corresponds to the most probable site that interacts with ATP.

Since P2Y1's active sites interacting with ATP have been known, and there are probably some similarities in sequences and molecule structures between P2Y1 and P2Y12 (Table 4), we chose the ''aligned two sequences'' from NCBI BLAST output to perform the alignment [32]. And that we have used the algorithm of PHD as well as the algorithm of GOR to analysis the characteristic of P2Y12's sequence [33,34]. All of the second structure and the trans-membrane districts are listed in Tables 5 and 6. Moreover, two theoretical structures of P2Y12 and P2Y1 (PDB code: 1ddd) [35] have been compared to explore the potential active sites, especially in trans-membrane districts in P2Y12.

2.3. The docking of reagents to the model of P2Y12 receptor

Since the three predicted active sites of P2Y12 locate at intracellular domain, extracellular domain and in the trans-membrane region, respectively, we used the *Docking* module of InsightII 2000 (Biosym Technologies Inc., San Diego, CA, USA) to dock the ATP/ADP in such different sites separately. At the same time, we measured the non-bond energy including the Van Der Waals energy, electrical energy and the total energy to value the sites we have previously predicted. We did the docking of such two kinds of ADP receptor antagonist to our model to verify the possibility of the three different sites.

3. Results

3.1. Structure prediction and molecular modeling of P2Y12

Table 5 lists the result of secondary structure prediction of P2Y12 by GOR and the prediction of the likely trans-membrane district colored by different colors using the algorithm of PHD. There is difference in secondary structure prediction between GOR and PHD. Here, single letters ''H, E, T, and C'' represent ''helix'', ''sheet'', ''turns'', and ''coil'', respectively; four segments colored by rose, 1–29, 80–98, 160–191, and 256–282, indicate the outside region of P2Y12; four ones colored by light green, 55–58, 119–139, 213–237, and 301–342, mean the inside region. And the rest colored by orange yellow (30–54), yellow (59–79), dark blue (99–118), purple (140–159), offwhite (192–212), dark red (238–255), and green (283–300) in turn, display seven trans-membrane segments. We submitted the model to the Protein Data Bank. After several refinements according to the feedbacks of the PDB deposition, the constructed structure was finally accepted as a sound theoretical structure and got an PDB id as 1VZ1.

Fig. 1. Molecular modeling of P2Y12. Seven different colors show seven trans-membrane areas.

Table 4
The result of the alignment between P2Y12 and P2Y1

```
P2Y1:   58  PAVYILVFIIGFLGNSVAIWMFVFHMKPWSGISVYMFNLALADFLYVLTLPALIFYYFNK 117
            P +Y ++F +G + N +A+ +F F ++   S    +++ N   ++D L +LT P   I
P2Y12: 32  PLLYTVLFFVGLITNGLAMRIF-FQIRSKSNFIIFLKNTVISDLLMILTFPFKILSDAKL 90

P2Y1:  118 TDWIFGDAMCKLQRFIFHVNLYGSILFLTCISAHRYSGVVYPLKSLGRLKKKNAIYISVL 177
                  +C++    IF+  +Y SI FL  I+  RY      P K+          A  +SV+
P2Y12: 91  GTGPLRTFVCQVTSVIFYFTMYISISFLGLITIDRYQKTTRPFKTSNPKNLLGAKILSVV 150

P2Y1:  178 VWLIVVVAISPILFYSGTGVRKNKTITCYDTTSDEYLRSYFIYSMCTTVAMFCVPLVLIL 237
            +W  + +    P +  +     R       C     S+  L  + I +     V +F +  ++++
P2Y12: 151 IWAFMFLLSLPNMILTNRQPRDKNVKKCSFLKSEFGLVWHEIVNYICQV-IFWINFLIVI 209

P2Y1:  238 GCYGLIVRALIYKDLDNSPL----RRKSIYLVIIVLTVFAVSYIPFHVMKTMNLRARLDF 293
                CY LI + L     +     +     R+K      V I++ VF + ++PFH          AR+ +
P2Y12: 210 VCYTLITKELYRSYVRTRGVGKVPRKKVNVKVFIIIAVFFICFVPFHF-------ARIPY 262

P2Y1:  294 ---QTPAM--CAFNDRVYATYQVTRGLASLNSCVDPILYFLAGDTFRRRL 338
                QT   +   C    + ++    + T   L SLN+C+DP +YF      +FR   L
P2Y12: 263 TLSQTRDVFDCTAENTLFYVKESTLWLTSLNACLDPFIYFFLCKSFRNSL 312
```

Score: 97.4 bits (241); expect: 9E−19; identities: 73/290 (25%); positives: 132/290 (45%); gaps: 18/290 (6%).

Fig. 1 is a snapshot of P2Y12, whose seven trans-membrane areas are labeled by seven different colors, namely dark yellow, yellow, dark blue, purple, white, dark red, and green, respectively, in comparison with the secondary structure prediction by PHD.

Fig. 2 displays the comparison of P2Y1 (left) and P2Y12 (right). We colored the known active sites red in P2Y1 structure and compared it with our model of P2Y12, in which predicted sites were also colored red. The comparison could suggest the predicted sites lying in trans-membrane region are probably the real active sites. Such area as VGLITNGLAM (38–47) and RTRGVGKVPR (222–231). Then we superimposed our P2Y12 model to the published structure of P2Y1 (1ddd), and gain a RMS value as 1.73426, which showed the similarity of them to some extent.

3.2. The sequence analysis of P2Y12

The scoring matrix consists of 13 different proteins. Table 2 shows the 10-peptide motifs of 13 proteins by CLUSTAL W

Table 5
The result of the prediction of the second structure of P2Y12 by GOR

garnier plot of /usr/tmp/2709448.sca, 342 aa; DCH = 0, DCS = 0

>/usr/tmp/2709448 [Unknown form], 342 bases, AD48D2D1 chec

. 10 . 20 . 30 . 40 . 50 . 60

MQAVDNLTSAPGNTSLCTRDYKITQVLFPLLYTVLFFVGLITNGLAMRIFFQIRSKSNFI

HHEEEEECCCTTTTEEEETTTTEEEEEEEEEEEEEEEECCCCCCEEEEECTTTEECTHH

. 70 . 80 . 90 . 100 . 110 . 120

IFLKNTVISDLLMILTFPFKILSDAKLGTGPLRTFVCQVTSVIFYFTMYISISFLGLITI

EEETCCCHHHEEEEEHHHHHHHHHTTTTCCCTEEEEEEEEEEEEEEETEEEEECEEEE

. 130 . 140 . 150 . 160 . 170 . 180

DRYQKTTRPFKTSNPKNLLGAKILSVVIWAFMFLLSLPNMILTNRQPRDKNVKKCSFLKS

ETTTTTCETTTTCCCTCHHHHHEEEEEHHHHHEHCCCCTEEEETECTTTTTTTEEEHEHC

. 190 . 200 . 210 . 220 . 230 . 240

EFGLVWHEIVNYICQVIFWINFLIVIVCYTLITKELYRSYVRTRGVGKVPRKKVNVKVFI

HHHHHHHHTTTTTEEEEEECTTEEEEEEEEEEEEEETTTEEEETTTTEEETHHHHEEEEE

. 250 . 260 . 270 . 280 . 290 . 300

IIAVFFICFVPFHFARIPYTLSQTRDVFDCTAENTLFYVKESTLWLTSLNACLDPFIYFF

EEEEEEETTCCTTTTTCTTCCTTTTTEEETHHHHHHHHHHHHHHHHHTCTTTTCEETEEEE

. 310 . 320 . 330 . 340

LCKSFRNSLISMLKCPNSATSLSQDNRKKEQDGGDPNEETPM

ETTTTTTTTEEEEECTTCCEEEHHCCTTTTTTTCCCCCCCHH

Residue totals (percent): H: 61 (18.7%); E: 141 (43.3%); T: 91 (27.9%); C: 49 (15.0%).
H: helix; E: sheet; T: turns; C: coil.

Note. Different color segments of P2Y12 by PHD. Here, four segments colored by rose color, 1–29, 80–98, 160–191, and 256–282, indicate the outside region of P2Y12; four ones colored by light green, 55–58, 119–139, 213–237, and 301–342, mean the inside region. And the rest colored by orange yellow (30–54), yellow (59–79), dark blue (99–118), purple (140–159), offwhite (192–212), dark red (238–255), and green (283–300), respectively, display seven trans-membrane segments. The four motifs underlined figure the predictive ATP-binding sites of P2Y12 by the scoring matrix. The letters shadowed means the potential ATP-binding sites of P2Y12 in comparison with P2Y1.

analysis and LPC analysis. Table 3 displays the scoring matrix of 10-peptide motif by running our scoring program and lists the score of each amino acid at each position. The capital letters in the first row of Table 3 points out amino acid residues consisting of the scoring matrix. Gln residue does not appear in the 13 sequences, so our amino acids are 19 totally. So the 10×19 matrix could be used to score an unknown protein's sequence to estimate if it possesses ATP-binding sites.

Actually, we scored the P2Y12's sequence by using the scoring program as follows: 7 7 5 9 6 11 9 8 12 7 17 11 4 1 5 10 11 9 11 3 3 8 9 3 2 7 15 6 2 9 17 7 9 3 11 12 2 18 3 12 14 2 10 2 9 8 5 6 5 7 6 9 10 6 7 4 5 5 10 16 4 3 9 11 6 2 6 6 6 6 8 5 13 10 4 4 4 6 8 7 14

Table 6
Intermolecular energies when docking the reagents to P2Y12 at three different areas

Compound	Energy (kcal)	Outside region	Trans-membrane	Inside region
ATP	Van der waals	−5.90174	−11.9444	−3.25605
	Elect	−0.46583	10.50171	−0.38125
	Total	−6.36757	−1.4369	−3.6373
ADP	Van der waals	−5.0863	−10.7749	−5.00521
	Elect	−1.6235	10.621	0.919245
	Total	−6.63213	−0.1539	−4.08597
Ticlopidine	Van der waals	−11.9444	−2.7659	−5.7521
	Elect	1.50171	1.34906	3.47214
	Total	−10.4427	−1.41981	−2.27997
Clopidogr	Van der waals	−5.00521	−3.76538	−5.27119
	Elect	0.919245	5.31247	3.21746
	Total	−4.05597	1.54709	−2.05372

5 12 10 6 24 7 13 5 8 16 9 6 11 7 7 8 7 6 8 6 5 6 12 6 9 7 10 11 4 9 12 4 13 1 9 7 8 12 10 5 5 7 13 8 5 8 6 8 8 7 3 8 3 6 13 10 20 11 4 8 8 6 14 6 9 3 4 7 3 2 7 5 8 9 3 6 4 8 5 3 6 9 7 4 11 8 5 6 10 6 6 8 6 12 13 10 7 3 13 8 4 3 6 4 8 12 2 3 6 7 2 3 6 7 10 7 9 4 2 10 10 4 9 7 9 9 5 11 6 10 10 6 11 11 8 13 5 15 19 7 18 3 15 10 7 11 8 10 5 5 6 8 10 8 1 2 8 10 10 9 5 4 3 8 4 6 4 4 1 6 8 3 6 11 12 10 7 4 6 6 10 8 4 3 7 11 5 10 11 8 8 4 12 8 9 9 6 8 5 6 8 7 7 4 3 6 4 6 2 6 6 4 8 7 6 7 6 6 7 5 7 5 7 5 5 10 7 6 4 10 9 7 5 7 11 6 2 6 7 6 7 7 3 7 8 6 10 7 11 12.

Each number denotes the similarity between a sequence of 10 amino acids and the sequences that constitute the matrix. And we got scores of every 10 amino acids out of the P2Y12's sequence, picking out the highest ones out of them. Within the scores it is easy to find out that the highest four numerals are 38th (24), 139th (20), 222nd (19) and 224th (18). They denote the sequence of 38–47, 87–96,139–148, and 222–231, respectively. Hence these four fragments are the most probable to be the interaction sites. Their sequences are VGLITNGLAM (38–47, 18 scores), LGTGPLRTFV (87–96, 24 scores), LGAKILSVVI (139–148, 20 scores), and RTRGVGKVPR (222–231, 19 scores), respectively. And there are two motifs in the trans-membrane (TM) region, namely VGLITNGLAM (TM1) and LGAKILSVVI (TM4); whereas LGTGPLRTFV and RTRGVGKVPR locate apart the second extracellular region and the third intracellular region. We show them in underlined letters of P2P12 in Table 5.

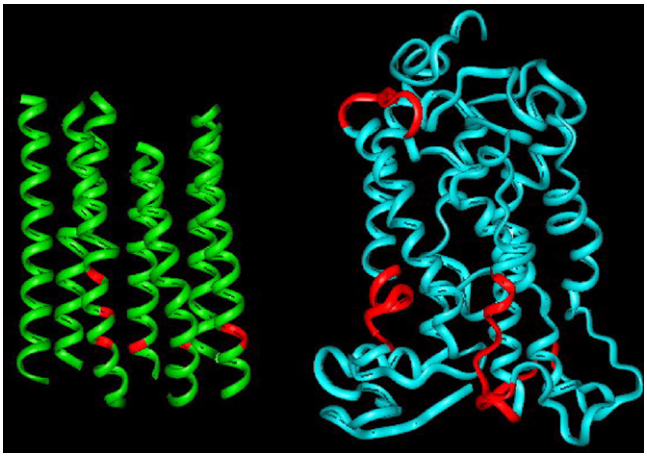

Fig. 2. The left is P2Y1 showed in green ribbon; in which the known ATP-binding sites are colored red. The right is P2Y12 colored in cyan ribbon whose four ATP-binding sequences predicted by the scoring program are labeled in red.

Table 4 lists the result of the alignment between P2Y12 and P2Y1 (PDB code: 1ddd) [35], and the identity is 25% but the positives is up to 45%. The known active sites in P2Y1 are labeled in red in Table 4, which are Arg131, Thr224-Thr225, Lys283, Gln310, Arg313, and Ser317. The corresponding residues in contact are concentrated in three dispersed regions of human P2Y12: Ser101, Cys194-Gln195, and the span from 281 to 288 (specially Glu281, Leu284, and Ser288), but in shortage of the corresponding residue with Lys283. These sites locate TM3, TM5, and TM7 in turn, which near the intracellular regions. And the letters shadowed in Table 5 means the potential ATP-binding sites of P2Y12 in comparison with P2Y1. And Ser101 lies at the 10-peptide motif LRTFVCQVTS (92–101, 16 scores), Cys194-Gln195 locates at a motif of IVNYICQVIF (189–198, 12 scores), and the span from 281 to 288 stands at a motif of LFYVKESTLW (276–285, 12 scores).

The result of alignment by BLAST between P2Y12 and bovine rhodopsin (PDB code: 1HZX) [14] shows that the length of two sequences aligned is 340, but the number of the amino acid residues actually aligned is 311; the percent of the sequences that are exactly the same is 15%, while the percent of the similarity is 29%. To increase the accuracy of the alignment, we gained the concrete result using the CLUSTAL W. Table 1 displays the sequence alignment between P2Y12 and bovine rhodopsin using the CLUSTAL. Using the algorithm of GOR, we get the result of the prediction of the secondary structure of P2Y12 in Table 5. These helped to construct the structure of P2Y12 by homologous modelling.

3.3. Interaction of some reagents with P2Y12

Since the P2Y12 can both interact with ATP and ADP, we deduce a conclusion from the predictive ATP-binding sites of P2Y12 that the ADP-binding sites of P2Y12 may be the same as ATP-binding sites. We suggest that some P2Y12 antagonists, such as ticlopidine and clopidogrel, would block ADP

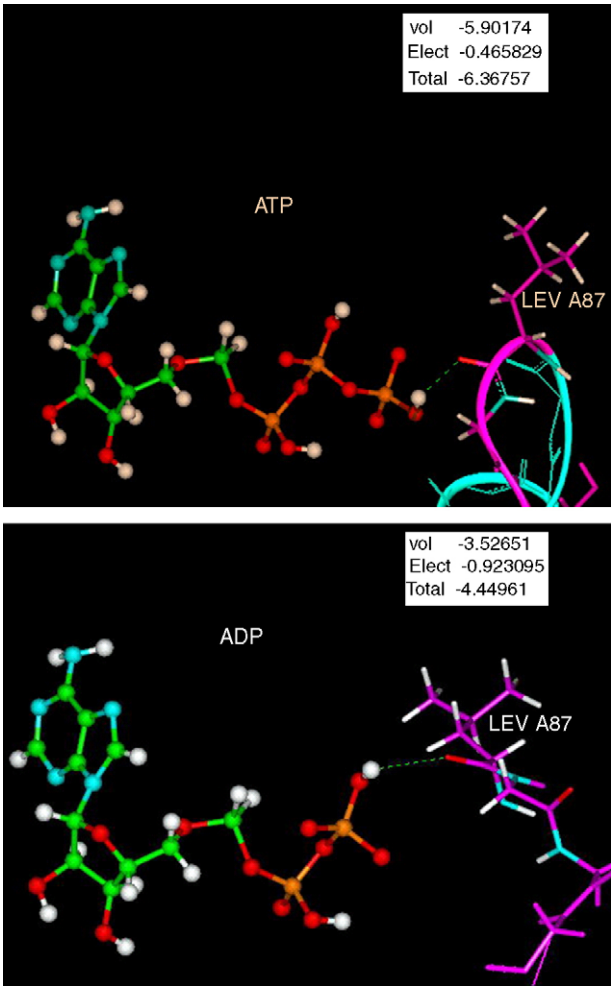

Fig. 3. Outside region. ATP (left) and ADP (right) are showed in ball-stick, and the P2Y12 showed in ribbon. The predicted active sites LGTG are colored in mauve. Left: ATPs hydroxyl hydrogen of P2 interaction with amide oxygen of LEU 87 of p2y12. Right: ADPs hydroxyl hydrogen of P1 interaction with amide oxygen of LEU 87 of p2y12.

interacting with its receptor P2Y12 by binding the same sites that may lie at three different areas, namely extracellular, transmembrane, and intracellular region. By calculating the intermolecular energies, we found that P2Y12 would interact with its antagonists by phosphate group rather than by adenosine, which means that the stronger polarity effects the interaction. At the same time, we speculated that P2Y12 would interact with ATP by Ser100 (TM3), Cys193-Gln194 (TM5), Glu280, Leu283, and Ser287 (TM7) based on the model of P2Y1's interacting with ATP (PDB code: Iddd) [35].

Table 6 lists the intermolecular energies when docking the reagents, such as ATP, ADP, ticlopidine, and clopidogr, to P2Y12 at three different areas.

Fig. 3 displays ATP (left) and ADP (right) interacting with P2Y12 in its "head area", which is the extrecellular region. ATP and ADP are showed in ball-stick, and P2Y12 is showed in ribbon; the predicted active sites (LGTG, 86–89) are colored by mauve line, while hydrogen bonds are colored by green dash. ATP formed a hydrogen bond by its hydroxyl hydrogen of terminal phosphate group (P2) with the amide oxygen of LEU 87 of P2Y12. Similarly, ADP formed a hydrogen bond by its hydroxyl hydrogen of terminal phosphate group (P1) with the amide oxygen of LEU 87.

Fig. 4 displays ATP (left) and ADP (right) interacting with P2Y12 in its "middle area", namely the trans-membrane region. There are two active sites of P2Y12 colored by red interacting with ATP by hydrogen bonds. ATP formed a hydrogen bond by its N6 of adenosine with the amide oxygen of ASN 43 of P2Y12, while P2Y12 formed double hydrogen bonds by the hydroxyl oxygen of its SER 145 with the hydroxyl hydrogen of P2 and the hydroxyl hydrogen of P of ATP, respectively. And ADP analogously formed a hydrogen bond by its N6 of adenosine with the amide oxygen of ASN 43; ADP formed another hydrogen bond by its hydroxyl hydrogen of P1 with the hydroxyl oxygen of SER 145.

Fig. 5 displays ATP (left) and ADP (right) interacting with P2Y12 in its "bottom area", namely the intracellular region. The predicted active sites LGAKILSVVI (139–148) of P2Y12 are showed in mauve ribbon. ATP formed a hydrogen bond by its hydroxyl hydrogen of P2 with the amide oxygen of GLY 140 of P2Y12. But there are two active sites of P2Y12 colored by red interacting with ADP by hydrogen bond. ADP formed a hydrogen bond by its hydroxyl hydrogen of P1 with the amide oxygen of GLY 140, while ADP formed a hydrogen bond by its hydroxyl oxygen of P with terminal amide hydrogen of LYS 142 of P2Y12.

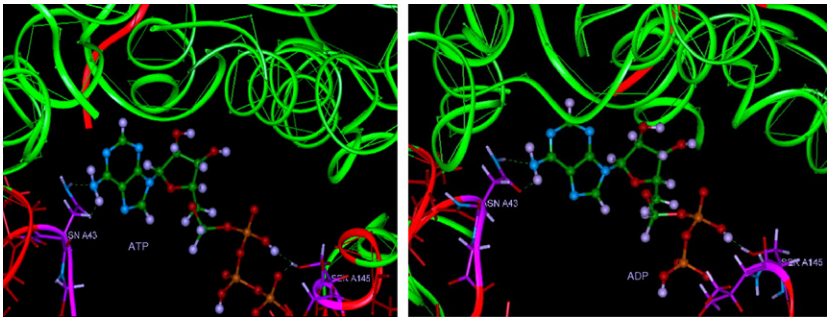

Fig. 4. Trans-membrane area. Left: ATP (left) and ADP (right) are showed in ball-stick, and the two active sites are showed in red ribbon. Left: one hydrogen bond was formed by amide hydrogen of ASN 43 with N6 of ATP; two were formed by the hydroxyl hydrogen of P2 of ATP, hydroxyl hydrogen of P of ATP and the hydroxyl oxygen of SER 145 of p2y12, respectively. Right: hydrogen bonds are formed by amide hydrogen of ASN 43 with N6 of ATP, the amide hydrogen of N6 of ADP with amide oxygen of ASN 43; and the hydroxyl hydrogen of P1 of ADP with the hydroxyl oxygen of SER 145 of p2y12.

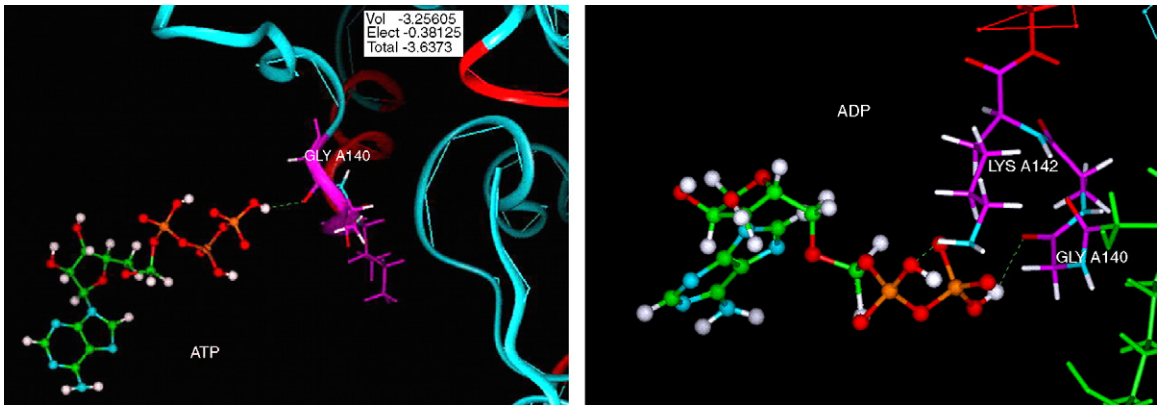

Fig. 5. Inside region. Left: ATP (left) and ADP (right) are showed in ball-stick, and the active sites LGAKILSVVI (139–148) are showed in red ribbon. Left: hydrogen bond is formed by the hydroxyl hydrogen of P2 of ATP with amide oxygen of GLY 140 of p2y12. Right: hydrogen bonds are formed by the hydroxyl hydrogen of P1 of ADP with amide oxygen of GLY 140 of p2y12, and hydroxyl oxygen of P of ADP with terminal amide hydrogen of LYS 142 of p2y12.

We have known that ticlopidine as well as clopidogrel acts as ADP receptor antagonist for inhibiting platelets aggregation [5]. The mechanism may be verified in our model of docking these two compounds to P2Y12 in predicted areas. Fig. 6 displays ticlopidine (upper) and clopidogr (lower) interacting with P2Y12 in three different areas, namely ''head area'' (left), ''middle area'' (middle), and ''bottom area'' (right), respectively. Ticlopidine and clopidogrel are showed in stick-and-ball, while all the interactive amino acids were showed in sticks with different colors to tell the different atoms. Similar to ATP/ADP, ticlopidine can form hydrogen bonds by its nitrogen atom with the amide oxygen of LEU 87 of P2Y12 (''head area''), with the amide oxygen of ASN 43 (''middle area''), and with amide oxygen of GLY 140 (''bottom area''), respectively. And clopidogrel can form hydrogen bonds by its nitrogen atom with the amide oxygen of LEU 87 of P2Y12 (''head area''), double

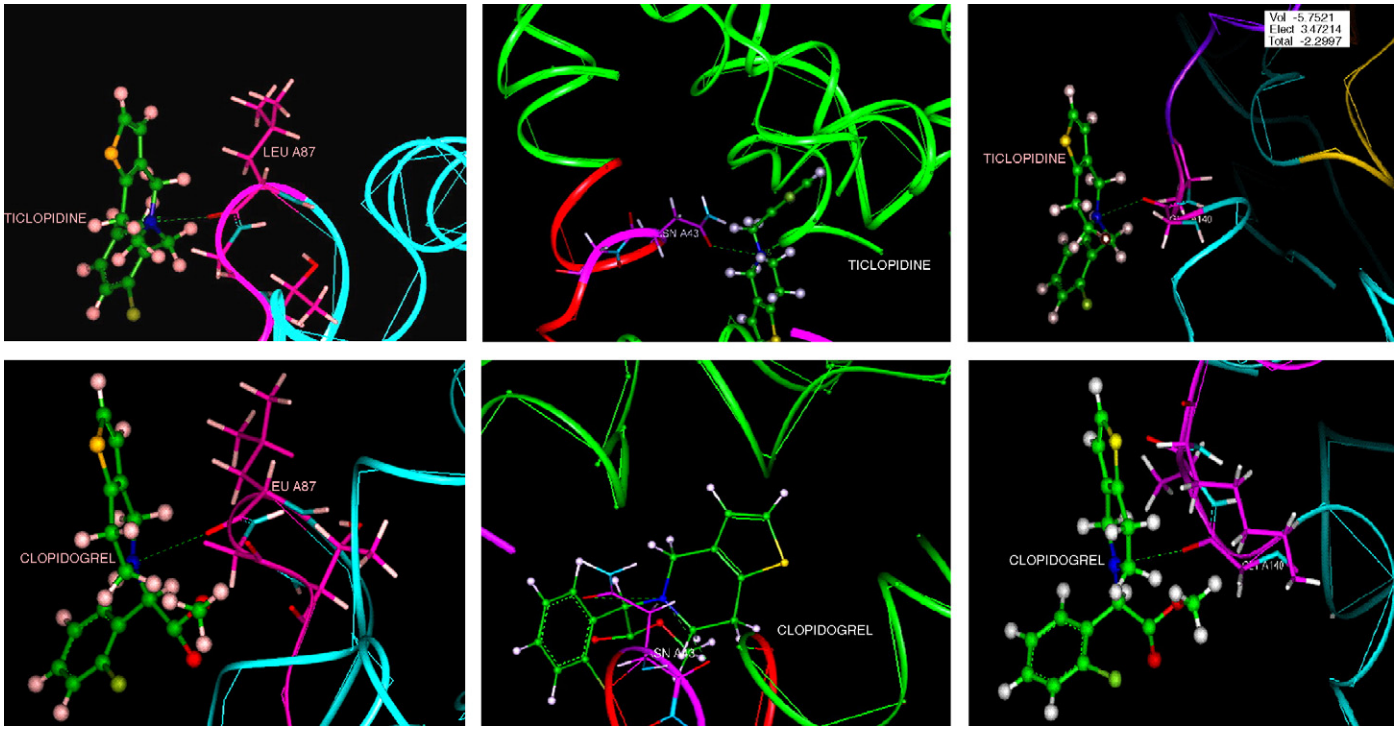

Fig. 6. Upper: the details of ticlopidine's interacting to different areas of p2y12. Left: showed that outside of the cell, there is a hydrogen bond forming between ticlopidine's nitrogen and amide oxygen of LEU 87 of p2y12, which showed in green dashed line. Middle: showed the condition in trans-membrane. There was a hydrogen bond forming between ticlopidine's nitrogen and amide oxygen of ASN 43. Right: showed that inside of the cell, a hydrogen bond formed between ticlopidine's nitrogen with amide oxygen of GLY 140 of p2y12. The ticlopidine was showed in stick-and-ball, while all the interactive amino acids were showed in sticks with different color to tell the different atoms. Lower: the details of clopidogrel's interacting to different areas of p2y12. Left: showed that outside of the cell, there is a hydrogen bond forming between clopidogrel's nitrogen and amide oxygen of LEU 87 of p2y12, which showed in green dashed line. Middle: showed the condition in trans-membrane. There are two hydrogen bonds forming by clopidogrel's nitrogen with amide oxygen of ASN 43 and hydroxyl oxygen of it, respectively. Right: showed that inside of the cell, a hydrogen bond formed by clopidogrel's nitrogen with amide oxygen of GLY 140 of p2y12. The clopidogrel are showed in stick-and-ball, while all the interactive amino acids are showed in sticks with different color to tell the different atoms.

with the amide oxygen and the hydroxyl oxygen of ASN 43 (''middle area''), and with amide oxygen of GLY 140 (''bottom area''), respectively.

The result of the intermolecular energy between all predicted active sites of P2Y12 and the four ligands: ATP, ADP, ticlopidine and clopidogrel have been calculated. The result was listed in Table 6. The Hydrogen bonds forming between the receptors and atoms on those amino acids in predicted sites is considered to bring down the total energy and stabilize the complexes.

4. Discussion

It has been known that structural information increases exponentially with prediction accuracy, revealing that even marginal gains in the performance of secondary structure prediction algorithms are important for the accuracy of structural information. We observe that different kinds of secondary structure prediction outputs (single-state prediction, single-state prediction with a confidence index, and three-state probability prediction) do not differ greatly in the amount of structural information they yield, so long as the methods formulated in this work to generate propensity distributions are applied appropriately [32]. It has common sense to constitute a scoring program with a matrix with sequences that have been established. Therefore, in theory, it could predict any protein whether it interacts with ATP and reveal the possible active sites. However, it is accustomed that the active sites are more than one. What is more, one matrix could predict only some diagnostic sites rather than all likely sites. Hence the choice of sequences that constitute the matrix still needs improving. It is obvious comparing the 13 proteins' active sites to find out that the length of one or two sites habitat of nearly each protein is about 10-peptide fragments. That is the reason why we choose a fragment of 10 amino acid of each protein that locates in the active sites habitat to constitute the matrix, and get good result. However such a choice remains rough, and the arbitrary has not been well controlled. Obviously, better results will be achieved after further improvement.

It could be found out that except for the last trans-membrane district, the six districts tally well with the 3D model, which shows an α helix. But the seventh trans-membrane district shows many corners in GOR, so it could be certain that such sequence inclines not to form a normal helix. Since other secondary structures of the protein predicted by GOR tally well with 1VZ1, it can be concluded that 1VZ1 probably has the ability to show the true 3D structure of the P2Y12. We colored the four most likely active sites in Fig. 2 in red. And we find that except that the sequence LGTGPLRTFV (87–96) locates in the loop between the second and third trans-membrane districts, the rest three fragments, VGLITNGLAM (38–47), LGAKILSVVI (139–148), and RTRGVGKVPR (222–231), all locate in the helix at the intracellular region. Since 87–96's score is the highest (24 scores), we notice that it locates in the loop outside the membrane, therefore its potentiality to be a active site has been confirmed considering the spatial factors. The scoring of this fragment of sequence is 24, out of which the first four-peptide LGTG solely gain 20 scores. This is surely the main contributor of the prediction. And in docking, a Hydrogen bond has been formed by ADP/ATP and LEU 87, which suggests the most likely site among the 10 amino acid residues. The second highest score winner LGAKILSVVI (139–148) also has a potential to be at least, one of the real sites because it also has few spatial obstacle. And after docking analysis, we could accept it as a likely active site for its lower intermolecular energy. A Hydrogen bond has been form by ADP/ATP and GLY 140, which suggests the most likely site among the 10-peptide motif. But as stated previously, since the known active sites in P2Y1 lie in the trans-membrane region and their similarities in structure and characteristic, we considered the VGLITNGLAM (38–47) and the former half of LGAKILSVVI (139–148), which locate in the ''middle'' of the molecule in trans-membrane area, as putative active sites. Maybe the total molecular energy has been brought down for the relatively higher electrical energy, however, there were many more hydrogen bonds forming with amino acids (there were four hydrogen bonds between ATP and ASN 43, SER 145; three hydrogen bonds between ADP and ASN 43, SER 145) in that area which have indicated more interacting sites there. And we did not show the hydrogen bonds forming by ADP/ATP and other amino acids that have not been involved in the two areas mentioned above, namely VGLITNGLAM (38–47) and the former half of LGAKILSVVI (139–148), we think that there are probably other interacting sites in the trans-membrane district like the condition of P2Y1.

There have been reports about the P2Y12 serving as an ADP and ATP receptor in platelets aggregation. And indeed, the roles of ADP and ATP in platelet aggregation have been fully investigated [5,7]. We docked ADP and ATP to P2Y12, respectively, and found the intermolecular energy verify the mechanism that ADP interacts with P2Y12 as well as P2Y1, inducing the platelet aggregation. However, as an ATP/ADP receptor the P2Y12 seems to show no obviously different affinity between them.

It is reported that the P2Y12 receptor is a well-established target of antithrombotic drugs such as clopidogrel. Some small compounds that have similar structures with ticlopidine as well as clopidogrel have been tested to show antiplatelet activity. The mechanism is that they could inhibit ADP receptor by interacting with those receptors as P2Y1 [5]. ADP is structurally similar to ATP, we speculate that these compounds having antiplatele activity would also have the ability to interact with P2Y12. To confirm our prediction of these active sites we firstly docked the known ticlopidine and clopidogrel to the model of P2Y12, in each likely active area, respectively. We are glad to find that the two compounds show similar affinities to P2Y12. Hydrogen bonds were found forming between P2Y12's probable active sites and the N of these compounds, which may greatly stabilize the complexes. Besides in the trans-membrane area, it seems that these two did not interact with so many amino acids as the ADP/ATP did, and forming less hydrogen bonds. Obviously, the intermolecular energy at this area also has been higher than the condition of ADP/ATP. However, totally it tallies well with the mechanism established

before. Secondly, we use the most active four kinds of small compounds to dock with P2Y12, which have been found to interact with ADP in our former research [36]. The energy results were approval to our speculation, and comparatively lower than other compounds. But because of the limited time, we adopted LEU 87 as the main interaction sites to do the docking. Our result suggests that these small compounds may also interact with ATP receptor P2Y12 in the process of platelets aggregation and further influence the activity of antiplatelet. The ATP has been found involving in regulation of Na/K–ATPase that regulate the [Ca] incremant through the P2Y receptors [37,38]. Our model may be a suspend of that. It has been found that in giant cells P2Y2 receptor transcripts are not present at the surface of cells as functional receptors, and ATP-induced effects on resorption, following direct osteoclastic activation are mediated by a P2 receptor other than the P2Y2 subtype, hence some little molecule such as nucleotide may interact with a complement of P2 receptor to influence the remodeling process [39]. As to the more detailed mechanism and that about P2 receptor such as signaling, there is still much to do in this field of research. Researchers have found interplay between P2Y1, P2Y12 and P2X1 receptors in the activation of megakaryocyte cation influx currents by ADP; evidence that the primary megakaryocyte represents a fully functional model of platelet P2 receptor signaling [40,41]. It reminds us that maybe more compounds and proteins from different cells are involved in platelet activity including some other marrow cells or blood cells.

Since the P2 receptor antagonists have been broadly used in clinic and for new drugs, the idea is put forward that combinations could improve efficacy with diminished hemorrhagic risk. Our results could have sense to elaborate the details in the procedure of blood coagulation, and analogues of ticlopidine may worth further tests to investigate the potential new target of drugs.

Acknowledgement

This project was supported by NSFC (Nature Science Fund of China, Nos. 30171094 and 30271497).

References

[1] C. Gachet, B. Hechler, The platelet P2 receptors in thrombosis, Semin. Thromb. Hemost. 31 (2) (2005) 162–167.
[2] B. Hechler, M. Cattaneo, C. Gachet, The P2 receptors in platelet function, Semin. Thromb. Hemost. 31 (2) (2005) 150–161.
[3] C.J. Foster, D.M. Prosser, J.M. Agans, Y. Zhai, M.D. Smith, J.E. Lachowicz, F.L. Zhang, E. Gustafson, F.J. Monsma Jr., M.T. Wiekowski, S.J. Abbondanzo, D.N. Cook, M.L. Bayne, S.A. Lira, M.S. Chintala, Molecular identification and characterization of the platelet ADP receptor targeted by thienopyridine antithrombotic drugs, J. Clin. Invest. 107 (12) (2001) 1591–1598.
[4] T. Müller, S. Rahmann, M. Rehmsmeier, Non-symmetric score matrices and the detection of homologous transmembrane proteins, Bioinformatics 17 (Suppl.) (2001) 182–189.
[5] A.A. Weber, S. Reimann, K. Schror, Specific inhibition of ADP-induced platelet aggregation by clopidogrel in vitro, Br. J. Pharmacol. 126 (2) (1999) 415–420.
[6] P. Sabala, R. Czajkowski, K. Przybylek, K. Kalita, L. Kaczmarek, J. Baranska, Two subtypes of G protein-coupled nucleotide receptors, P2Y(1) and P2Y(2) are involved in calcium signalling in glioma C6 cells, Br. J. Pharmacol. 132 (2) (2001) 393–402.
[7] P. Savi, P. Beauverger, C. Labouret, M. Delfaud, V. Salel, M. Kaghad, J.M. Herbert, Role of P2Y1 purinoceptor in ADP-induced platelet activation, FEBS Lett. 422 (1998) 291–295.
[8] M.H. Pausch, M. Lai, E. Tseng, J. Paulsen, B. Bates, S. Kwak, Functional expression of human and mouse P2Y12 receptors in Saccharomyces cerevisiae, Biochem. Biophys. Res. Commun. 324 (1) (2004) 171–177.
[9] K.C. Chou, Review: structural bioinformatics and its impact to biomedical science, Curr. Med. Chem. 11 (2004) 2105–2134.
[10] K.C. Chou, Insights from modelling the 3D structure of the extracellular domain of alpha7 nicotinic acetylcholine receptor, Biochem. Biophys. Res. Commun. 319 (2004) 433–438.
[11] K.C. Chou, Modelling extracellular domains of GABA-A receptors: subtypes 1, 2, 3, and 5, Biochem. Biophys. Res. Commun. 316 (2004) 636–642.
[12] K.C. Chou, Coupling interaction between thromboxane A2 receptor and alpha-13 subunit of guanine nucleotide-binding protein, J. Proteome Res. 4 (2005) 1681–1686.
[13] K.C. Chou, Prediction of G-protein-coupled receptor classes, J. Proteome Res. 4 (2005) 1413–1418.
[14] D.C. Teller, T. Okada, C.A. Behnke, K. Palczewski, R.E. Stenkamp, Advances in determination of a high-resolution three-dimensional structure of rhodopsin, a model of G-protein-coupled receptors (GPCRs), Biochemistry 40 (2001) 7761–7772.
[15] J. Yang, C.Q. Liu, Molecular modeling on human CCR5 receptors and complex with CD4 antigens and HIV-1envelope glycoprotein gp120, Acta Pharmacol. Sin. 20 (1) (2000) 29–34.
[16] S.Q. Liu, J. Yang, C.L. Bai, C.Q. Liu, System analysis of the energies of the triple base triplets, Am. J. Human Genet. 69 (4) (2001) 2938, Suppl.
[17] J. Yang, Y. Leng, J. Bao, Application of RNA–DNA duplex base triplets to antisense drugs, Am. J. Biochem. Biotechnol. 1 (2) (2005) 74–84.
[18] Y.K. Yosef, S. Vladimir, R. Alexander, E. Marvin, A consensus-binding structure for adenine at the atomic level permits searching for the ligand site in a wide spectrum of adenine-containing complexes, Proteins: Struct. Funct. Genet. 52 (3) (2003) 400–411.
[19] U. Schulze-Gahmen, H.L. De Bondt, S.H. Kim, High-resolution crystal structures of human cyclin-dependent kinase 2 with and without ATP: bound waters and natural ligand as guides for inhibitor design, J. Med. Chem. 39 (1996) 4540–4546.
[20] J.H. Zheng, E.A. Trafny, D.R. Knighton, N.H. Xuong, S.S. Taylor, L.F. Teneyck, J.M. Sowadski, 2.2-Angstrom refined crystal-structure of the catalytic subunit of cAMP-dependent protein-kinase complexed with mnATP and a peptide inhibitor, Acta Crystallogr. D: Biol. Crystallogr. 49 (1993) 362–365.
[21] D.J. Owen, M.E. Noble, E.F. Garman, A.C. Papageorgiou, L.N. Johnson, Two structures of the catalytic domain of phosphorylase kinase: an active protein kinase complexed with substrate analogue and product, Structure 3 (1995) 467–482.
[22] H. Kack, K.J. Gibson, Y. Lindqvist, G. Schneider, Snapshot of a phosphorylated substrate intermediate by kinetic crystallography, Proc. Natl. Acad. Sci. U.S.A. 95 (1998) 5495–5500.
[23] R.M. Xu, G. Carmel, R.M. Sweet, J. Kuret, X. Cheng, Crystal structure of casein kinase-1, a phosphate-directed protein kinase, EMBO J. 14 (1995) 1015–1023.
[24] T.I. Zarembinski, L.-W. Hung, H.J. Mueller-Dieckmann, K.-K. Kim, H. Yokota, R. Kim, S.-H. Kim, Structure-based assignment of the biochemical function of a hypothetical protein: a test case of structural genomics, Proc. Natl. Acad. Sci. U.S.A. 95 (1998) 15189–15193.
[25] T.M. Larsen, M.M. Benning, I. Rayment, G.H. Reed, Structure of the bis(Mg2+)-ATP-oxalate complex of the rabbit muscle pyruvate kinase at 2.1 A resolution: ATP binding over a barrel, Biochemistry 37 (1998) 6247–6255.
[26] L.W. Tari, A. Matte, U. Pugazhenthi, H. Goldie, L.T. Delbaere, Snapshot of an enzyme reaction intermediate in the structure of the ATP-Mg2+-oxalate ternary complex of *Escherichia coli* PEP carboxykinase, Nat. Struct. Biol. 3 (1996) 355–363.

[27] E. Schmitt, L. Moulinier, S. Fujiwara, T. Imanaka, J.C. Thierry, D. Moras, Crystal structure of aspartyl-tRNA synthetase from *Pyrococcus kodakaraensis* KOD: archaeon specificity and catalytic mechanism of adenylate formation, EMBO J. 17 (1998) 5227–5237.

[28] M.C. O'Brien, K.M. Flaherty, D.B. McKay, Lysine 71 of the chaperone protein Hsc70 Is essential for ATP hydrolysis, J. Biol. Chem. 271 (1996) 15874–15878.

[29] E.H. Walker, M.E. Pacold, O. Perisic, L. Stephens, P.T. Hawkins, M.P. Wymann, R.L. Williams, Structural determinants of phosphoinositide 3-kinase inhibition by wortmannin, LY294002, quercetin, myricetin, and staurosporine, Mol. Cell. 6 (2000) 909–919.

[30] S. Vorobiev, B. Strokopytov, D.G. Drubin, C. Frieden, S. Ono, J. Condeelis, P.A. Rubenstein, S.C. Almo, The structure of non-vertebrate actin: implications for the ATP hydrolytic mechanism, Proc. Natl. Acad. Sci. U.S.A. 100 (2003) 5760–5765.

[31] R.C. Yu, P.I. Hanson, R. Jahn, A.T. Brunger, Structure of the ATP-dependent oligomerization domain of *N*-ethylmaleimide sensitive factor complexed with ATP, Nat. Struct. Biol. 5 (1998) 803–811.

[32] A.D. Solis, S. Rackovsky, On the use of secondary structure in protein structure prediction: a bioinformatic analysis, Sci. Direct Polym. 45 (2004) 525–546.

[33] V. Sobolev, A. Sorokine, J. Prilusky, E.E. Abola, M. Edelman, Automated analysis of interatomic contacts in proteins, Bioinformatics 15 (1999) 327–332.

[34] D.L. Wheeler, D.M. Church, S. Federhen, A.E. Lash, T.L. Madden, J.U. Pontius, G.D. Schuler, L.M. Schriml, E. Sequeira, T.A. Tatusova, L. Wagner, Database resources of the National Center for Biotechnology, Nucl. Acids Res. 31 (1) (2003) 28–33.

[35] A.M. Van Rhee, B. Fischer, P.J. Van Galen, K.A. Jacobson, Modelling the P2Y purinoceptor using rhodopsin as template, Drug Des. Discov. 13 (2) (1995) 133–154.

[36] J. Yang, W.Y. Hua, F.X. Wang, Z.Y. Wang, X. Wang, Design, synthesis, and inhibition of platelet aggregation for some 1-*o*-chlorophenyl-1,2,3,4-tetrahydroisoquinoline derivatives, Bioorg. Med. Chem. 12 (24) (2004) 6547–6557.

[37] S. Koizumi, Y. Saito, K. Nakazawa, K. Nakajima, J.I. Sawada, S. Kohsaka, P. Illes, K. Inoue, Spatial and temporal aspects of Ca2+ signaling mediated by P2Y receptors in cultured rat hippocampal astrocytes, Life Sci. 72 (2002) 431–442.

[38] A. Muscella, M.G. Elia, S. Greco, C. Storelli, S. Marsigliante, Activation of P2Y2 purinoceptor inhibits the activity of the Na+/K+–ATPase in HeLa cells, Cell. Signal. 15 (2003) 115–121.

[39] S. Berchtold, A.L. Ogilvie, C. Bogdan, P. Muhl-Zurbes, A. Ogilvie, G. Schuler, A. Steinkasserer, Human monocyte derived dendritic cells ezpress functional P2X and P2Y receptors as well as ecto-nucleotidases, FEBS Lett. 458 (1999) 424–428.

[40] W.B. Bowler, A. Littlewood-Evans, G. Bilbe, J.A. Gallagher, C.J. Dixon, P2Y2 receptors are expressed by Human osteoclasts of Giant cell tumor but do not mediate ATP-induced bone resorption, Bone 22 (3) (1998) 195–200.

[41] G. Tolhurst, C. Vial, C. Leon, C. Gachet, R.J. Evans, M.P. Mahaut-Smith, Interplay between P2Y(1), P2Y(12), and P2X(1) receptors in the activation of megakaryocyte cation influx currents by ADP: evidence that the primary megakaryocyte represents a fully functional model of platelet P2 receptor signaling, Blood 106 (5) (2005) 1644–1651.